



Calhoun: The NPS Institutional Archive
DSpace Repository

Theses and Dissertations

1. Thesis and Dissertation Collection, all items

1973

The wavelength spectrum shift of a
cavity-dumped argon laser-pumped
Rhodamine 6-G organic-dye laser.

Snyder, Gerald Warner.

Monterey, California. Naval Postgraduate School

<http://hdl.handle.net/10945/16869>

Downloaded from NPS Archive: Calhoun



Calhoun is the Naval Postgraduate School's public access digital repository for research materials and institutional publications created by the NPS community. Calhoun is named for Professor of Mathematics Guy K. Calhoun, NPS's first appointed -- and published -- scholarly author.

Dudley Knox Library / Naval Postgraduate School
411 Dyer Road / 1 University Circle
Monterey, California USA 93943

<http://www.nps.edu/library>

THE WAVELENGTH SPECTRUM SHIFT OF A
CAVITY-DUMPED ARGON LASER-PUMPED
RHODAMINE 6-G ORGANIC-DYE LASER

Gerald Warner Snyder

Library
Naval Postgraduate School
Monterey, California 93940

NAVAL POSTGRADUATE SCHOOL

Monterey, California



THESIS

THE WAVELENGTH SPECTRUM SHIFT OF A CAVITY-DUMPED
ARGON LASER-PUMPED RHODAMINE 6-G ORGANIC-DYE LASER

by

Gerald Warner Snyder

Thesis Advisor:

John P. Powers

September 1973

T156412

Approved for public release; distribution unlimited.

The Wavelength Spectrum Shift of a Cavity-Dumped
Argon Laser-Pumped Rhodamine 6-G Organic-Dye Laser

by

Gerald Warner Snyder
Lieutenant Commander, United States Navy
B. S., United States Naval Academy, 1964

Submitted in partial fulfillment of the
requirements for the degree of

ELECTRICAL ENGINEER

from the
NAVAL POSTGRADUATE SCHOOL
September 1973

ABSTRACT

The wavelength spectrum of a CW pumped Rhodamine 6-G organic dye laser is observed to shift approximately 150 Angstroms toward shorter wavelengths when pumped by 30 nsec pulses at a one megahertz repetition rate from a cavity-dumped Argon laser. Experimental evidence of the shift is presented, gain and rate equations are developed for a simplified dye laser model, and theoretical results are obtained for a computer simulation of the experiment. A comparison is made of the theoretical and experimental results and satisfactory agreement is obtained within the limits of the values of the parameters used and the assumptions made in formulating the model.

TABLE OF CONTENTS

I.	INTRODUCTION	5
II.	DYE LASER THEORY	8
	A. ORGANIC DYE PROPERTIES	8
	1. Energy Level Description	8
	2. Dye Laser Process	8
	B. DYE LASER MATHEMATICS	11
	1. Dye Laser Gain Equation	11
	2. Dye Laser Rate Equations	15
III.	EXPERIMENTAL PROCEDURES AND RESULTS	17
	A. EXPERIMENTAL SET UP	17
	B. EXPERIMENTAL PROCEDURES	17
	C. EXPERIMENTAL RESULTS	20
IV.	DYE LASER MODEL EVALUATION	25
	A. LITERATURE SURVEY	25
	B. GAIN AND RATE EQUATION PARAMETERS	27
	C. GAIN AND RATE EQUATION SOLUTIONS	32
	1. Solution Method	32
	2. Theoretical Results	33
V.	CONCLUSIONS	37
	A. EXPERIMENTAL AND THEORETICAL COMPARISON	37
	B. REMARKS	38
	APPENDIX A Computer Program Listing	39
	BIBLIOGRAPHY	54
	INITIAL DISTRIBUTION LIST	58
	FORM DD 1473	59

ACKNOWLEDGEMENT

I am grateful for the help and support of Professor John Powers of the U.S. Naval Postgraduate School. I also want to thank Jim Jernigan of Code 6043, U.S. Naval Weapons Center, China Lake, California for the use of equipment and technical advice.

I. INTRODUCTION

Man's quest for knowledge, inherent curiosity, and need for a tunable coherent source of light have rapidly advanced the development of the organic dye laser since stimulated emission was observed from Trivalent Uranium (a four level laser system) by Sorokin and Stevenson [1] in 1960.

Brock, et al. [2] in 1961 proposed that organic compounds could be used as a laser medium, but stimulated emission from an organic material was not observed until 1962 when Morantz, White and Wright [3] observed it from benzophenone and naphthalene imbedded in a glass matrix. This was followed in 1963 by the observation of stimulated processes from Eu-benzoylacetate by Lempicki and Samuelson [4].

Stimulated emission from an organic dye, however, was not accomplished until 1966 when it was observed by Sorokin and Lankard [5] from Chloroaluminum phthalocyanine dissolved in ethyl alcohol when pumped by a giant pulse ruby laser. Sorokin and Lankard [6] also reported in 1967 the first observed stimulated emission from flashlamp pumped Acridine Red, Rhodamine 6-G (the most common dye used in present day organic dye lasers), and Fluorescein. Schafer, Schmidt, and Volze [7] reported stimulated emission from several other organic dyes during this same time period while using the same basic procedure as Sorokin and Lankard [5], and they were the first to suggest that a dye laser operated on transitions from the excited singlet state to vibrational levels of the ground singlet state.

The feasibility of a continuous wave dye laser was discussed by Snavely [8] and was demonstrated by Snavely and Schafer [9] in 1969. CW operation was achieved in 1970 by Peterson, Tuccio and Snavely [10] and

Hercher and Pike [11] using an Argon ion laser as the pump source and Rhodamine 6-G as the organic dye.

The first CW dye lasers were only about one percent efficient. This has been raised to the present day level of thirty-five percent through the efforts of several groups of people including Hercher and Pike [12, 13], Kohn, Shank, Ippen and Dienes [14, 15], and Tuccio and Strome [16, 17].

The evolution of the dye laser has seen it constructed in many ways. The tunable distributed-feedback dye laser built by Shank, Bjorkholm and Kogelnik [18], the prism-dye laser constructed by Chandra, Takeuchi, and Hartmann [19], and the evanescent-field-pumped dye laser demonstrated by Ippen and Shank [20] are a few of the many sophisticated methods that have been used to obtain dye laser emission. The most common dye laser configuration, however, has the pump and dye laser cavities aligned with the beams coincident and the dye flowing perpendicular to the pump beam through a dye cell.

Several uses have been proposed for dye lasers. Bloom [21] has suggested its use for attenuation measurements on narrow-band absorption lines in molecular gases, and Sorokin, Lankard, Moruzzi and Hammond [22] have proposed using the dye laser for optical studies of rare-earth ions, photochemistry, and double-quantum absorption spectroscopy. The dye laser characteristics which make it exceptionally well suited to the above uses are its tunable range which can be as much as 1100 Angstroms from a single dye, and its narrow linewidth which is normally less than 0.5 Angstroms.

Uses for the dye laser which have already been published include infrared difference-frequency generation [23], megawatt tunable second harmonic and sum frequency generation [24], studies of the Sodium D

resonance lines by high resolution Spectroscopy [25], and detection of OH in the atmosphere [26]. Further uses of the dye laser are limited only by the interest and ingenuity of man.

In this work it has been observed that the output wavelength spectrum of a CW pumped Rhodamine 6-G organic dye laser shifts toward shorter wavelengths when pumped by short intense pulses from a cavity-dumped Argon laser. This shift to the green region of the visible wavelength spectrum is important in that the new spectrum can be matched to the wavelength response curve of a crystal to produce a tunable dye laser optical memory system. The new spectrum also provides the opportunity to investigate laser propagation in blue and green sea water over an appreciable wavelength range using a single dye.

The purpose of this thesis is to provide experimental results of the observed spectrum shift, to obtain a computer simulation of a dye laser model, and to compare experimental and theoretical results. Section II discusses dye laser theory based on energy level considerations and gives the development of the dye laser gain and rate equations for an assumed physical model. Section III presents experimental procedures and results and Section IV discusses the solution procedures and results of the theoretical model. Section V provides a comparison of experimental and theoretical results and conclusions. The computer program used to solve the dye laser model is listed in Appendix A.

II. DYE LASER THEORY

A. ORGANIC DYE PROPERTIES

1. Energy Level Description

A typical energy level diagram for an organic dye is shown in Figure 1. The reference level A is the electronic ground state of the molecular singlet state S_0 . S_1 and S_2 are the first and second excited singlet states, and T_1 and T_2 are the first and second excited triplet states. The small letters a and b indicate molecular vibrational energy levels and the primed letters indicate molecular rotational energy levels within a state. The typical separation of vibrational energy levels is 0.1 electron volts and that of rotational energy levels is 0.001 electron volts [27] so that each state may be viewed as a continuous band of energy.

2. Dye Laser Process

The dye laser process starts with the excitation of molecules from level A of S_0 to an upper vibrational or rotational level of S_1 . The excited molecules then decay very rapidly (10^{-10} - 10^{-13} sec) [28] by nonradiative internal conversion to B.

The excited molecule in B has three options. It may decay spontaneously to a or a' (called fluorescence), it may undergo a stimulated transition to a or a', or it may travel via intersystem crossing to the lower level of T_1 .

Fluorescence depends on the natural lifetime of B. The fluorescence spectrum of an organic dye is governed by the Franck-Condon principle [29] which states that preferred electron transitions are determined by the wave functions of the individual energy levels.

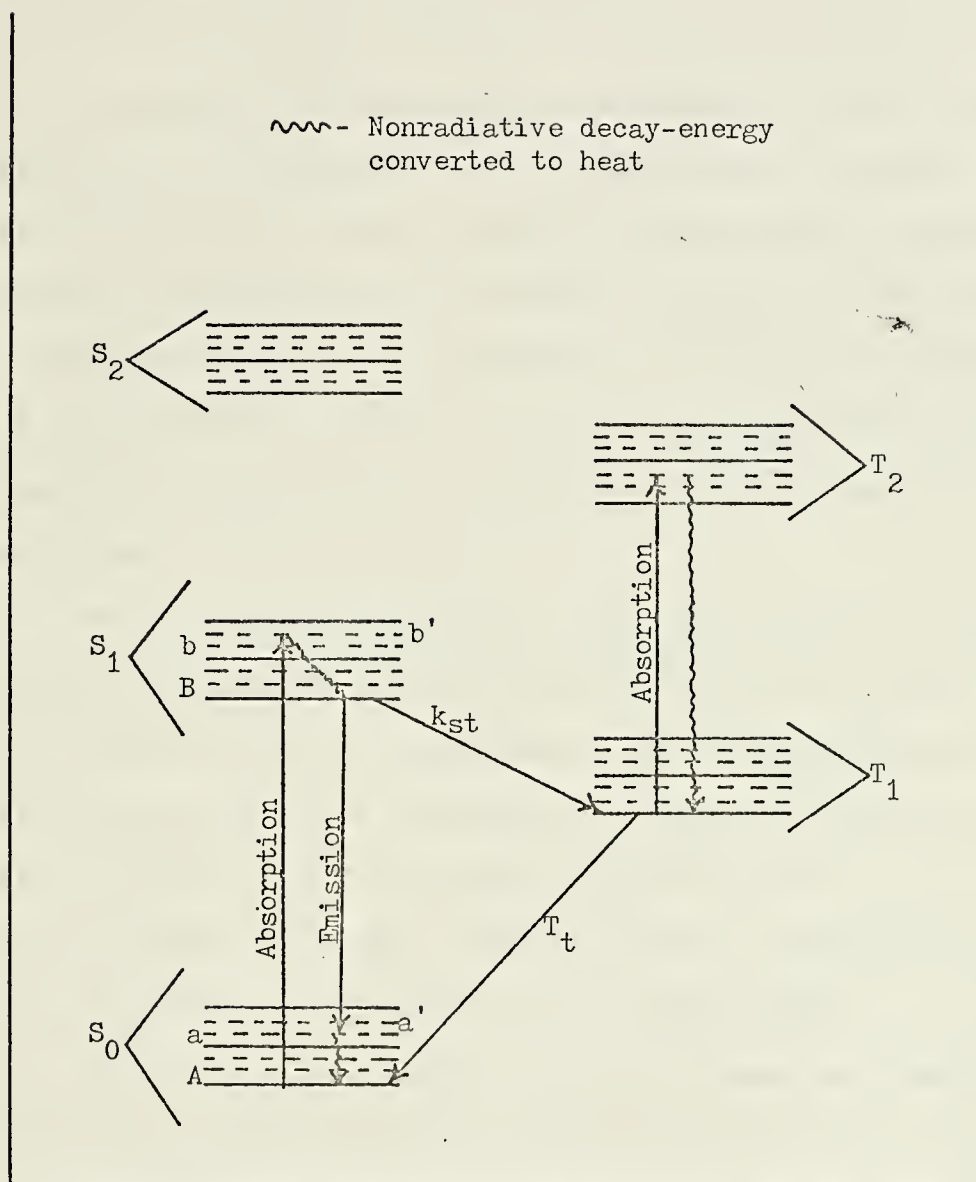


Figure 1: Organic dye energy levels.

Stimulated transition to a or a' can occur only if the excitation pulse is fast and intense enough to create a much larger than normal concentration of molecules in S_1 , called critical inversion, so that coherent emission may take place from the dye. The critical inversion as well as the emission wavelength are governed by losses in the dye laser system. Once the excited molecule reaches a or a' it decays nonradiatively to A.

Intersystem crossing is the least desirable transition for an excited molecule. The singlet state is characterized by opposite electron spins and the triplet state by parallel electron spins. As a result, according to the laws of quantum mechanics, the $S_1 - T_1$ transition is spin forbidden and is in fact approximately 10^{-6} [30] less probable than the $S_1 - S_0$ transition. However, the $S_1 - T_1$ transition does occur and is significant enough to have an important negative effect on the dye laser process.

The intersystem crossing rate time constant, k_{st}^{-1} , is generally much smaller than the T_1 state lifetime, T_t , therefore, state T_1 acts as a time dependent trap for dye molecules. This not only reduces the possible dye laser efficiency by removing dye molecules from the singlet system, but also, since the absorption spectrum of the $T_1 - T_2$ transition of an organic dye usually overlaps the dye fluorescence spectrum, another loss mechanism is added to the dye laser system. $S_1 - S_2$ absorption is possible but it is usually neglected because the fraction of molecules in S_1 needed to achieve critical inversion is very small [31].

Transitions to A are generally assumed to be from the lowest level of T_1 . These transitions may be either radiative, called phosphorescence, or, as is the situation for most organic dyes, nonradiative. The longer T_t is, the faster the dye pumping pulse has to be to excite

enough molecules to reach critical inversion before the T_1 trap prevents dye laser emission.

The T_1 trap problem has caused a lot of research to be done to find substances which will shorten T_t via collisions with molecules in T_1 . This action is called quenching and two very effective quenching agents are cyclooctatetraene (COT) and molecular oxygen.

B. DYE LASER MATHEMATICS

1. Dye Laser Gain Equation

The dye laser gain equation is a mathematical statement of the production and loss rates for photons in the laser cavity. Photons are produced by stimulated emission from the excited singlet state to the ground singlet state. Photons are lost by $S_0 - S_1$ and $T_1 - T_2$ absorption and by loss through extrinsic means such as output mirrors, optical surface scattering, etc. Photon production is also possible by stimulated emission from the excited triplet state but nonradiative decay is so rapid from this state to the lower triplet state that this source of photons can be neglected.

A simplified schematic diagram of a dye laser is shown in Figure 2. L_1 is the dye cell length, R_1 and R_2 are the input and output mirror reflectivities, T_1 and T_2 are the dye cell window transmittances, and n_0, n_1, n_2 , etc. are the photon densities at any time at the indicated positions of a round trip in the laser cavity. This particular cavity is used as the model for the following derivation of the gain equation.

The rate of photon production per unit length in the dye may be written as follows:

$$\frac{dn}{dl}_{\text{total}} = \frac{dn}{dl}_{\text{emission}} - \frac{dn}{dl}_{\text{absorption}} \quad (1)$$

The first term on the right hand side of (1) is photon production by stimulated emission and the second term is photon loss by singlet and triplet state absorption.

Yariv and Gordon [32] have shown that the expression for the transition rate caused by a monochromatic beam of light of wavelength λ is

$$\frac{dn}{dt}_e = \frac{N_s \lambda^4 E(\lambda) n(\lambda)}{8 \pi T_s \bar{n}^3} \text{ cm}^{-3} \text{ sec}^{-1} \quad (2)$$

where N_s is the population density of the excited singlet state, $n(\lambda)$ is the number of photons of wavelength λ per cm^3 of active medium, T_s is the excited singlet state lifetime, \bar{n} is the index of refraction, and $E(\lambda)$ is the fluorescence lineshape function normalized so that

$$\int_0^{\infty} E(\lambda) d\lambda = \phi = \text{quantum yield} = \frac{\text{photons emitted}}{\text{photons absorbed}}.$$

An expression for the first term of (1) can now be derived. Since

$$\frac{dn}{dt}_e = \frac{dn}{dl}_e \times \frac{dl}{dt} \quad \text{and} \quad \frac{dl}{dt} = \text{velocity} = \frac{c}{\bar{n}}$$

where c is the speed of light, it follows that

$$\frac{dn}{dl}_e = \frac{N_s \lambda^4 E(\lambda) n(\lambda)}{8 \pi c T_s \bar{n}^2} \quad (3)$$

The molecular extinction coefficient, which is the absorption cross-section for a single dye molecule, can be used to write the singlet and triplet absorption loss per unit length for (1). These terms are

$$\frac{dn}{dl}_{\text{singlet}} = n(\lambda) N_o \sigma_s(\lambda) \quad (4)$$

$$\frac{dn}{dl}_{\text{triplet}} = n(\lambda) N_t \sigma_t(\lambda) \quad (5)$$

where N_o and N_t are the population densities of the ground singlet and triplet states, and σ_s and σ_t are the wavelength dependent singlet and triplet absorption cross-sections.

Let

$$\sigma_e(\lambda) = \frac{\lambda^4 E(\lambda)}{8\pi c T_s \bar{n}^2}$$

and substitute (3), (4) and (5) into (1). This yields the total production rate of photons per unit length in the dye medium which is

$$\frac{dn}{dl}_{\text{total}} = n(\lambda) \sigma_e(\lambda) N_s - n(\lambda) \sigma_s(\lambda) N_o - n(\lambda) \sigma_t(\lambda) N_t. \quad (6)$$

Separation of variables of (6) and integration over the length of the dye cell with the boundary conditions that where $l = 0$, $n = n_1$, and where $l = L_1$, $n = n_2$, yields the solution

$$n_2 = n_1 \exp[\sigma_e N_s - \sigma_s N_o - \sigma_t N_t] L_1. \quad (7)$$

The n 's and σ 's are still wavelength dependent and from Figure 2 it can be seen that since the paths traveled by photons n_1 and n_5 are through the same medium but in opposite directions that (7) also holds for the relation between n_6 and n_5 .

It is obvious from Figure 2 that $n_1 = n_0 T_1$, $n_3 = n_2 T_2$, $n_4 = n_3 R_2$, $n_5 = n_4 T_2$, $n_7 = n_6 T_1$, and $n_8 = n_7 R_1$. Substitution of these relations consecutively into (7) gives the result

$$n_8 = n_0 \exp[\sigma_e N_s - \sigma_s N_o - \sigma_t N_t + \frac{1}{2L_1} \ln(R_1 R_2 T_1^2 T_2^2)] 2L_1. \quad (8)$$

Let $G(\lambda)$ be the equation in brackets in (8) and define it to be the gain. Then

$$n_8 = n_0 \exp[2 G(\lambda) L_1], \text{ and}$$

$$G(\lambda) = \sigma_e N_s - \sigma_s N_o - \sigma_t N_t + \frac{1}{2L_1} \ln[R_1 R_2 T_1^2 T_2^2] \quad (9)$$

which is the desired gain equation and is similar to the results obtained by Snively [8] and McColgin, et al. [33].

2. Dye Laser Rate Equations

The dye laser will lase at the value of λ where (9) is a maximum. To find this wavelength it is necessary to solve the state population density rate equations for the dye laser. These equations are

$$\frac{dN_s}{dt} = -\frac{1}{T_s} N_s + P(t)N_o \quad (10A)$$

$$\frac{dN_t}{dt} = -\frac{1}{T_t} N_t + k_{st}N_s \quad (10B)$$

$$\frac{dN_o}{dt} = -P(t)N_o + \left(\frac{1}{T_s} - k_{st}\right)N_s + \frac{1}{T_t} N_t \quad (10C)$$

$$N = N_o + N_s + N_t \quad (10D)$$

N is the total population density and (10D) is true only for an enclosed system undergoing no photochemical processes. N_t , N_o , and N_s are as defined for the gain equation, T_s and T_t are the lifetimes of the singlet and triplet states, k_{st} is the excited singlet to ground triplet intersystem crossing rate constant, and $P(t)$ is the optical pumping rate.

There are several assumptions made in writing the rate equations in the form of (10A), (10B), (10C) and (10D). These assumptions are:

(a) The number of molecules involved in intersystem crossing from the triplet to the singlet state is negligible.

(b) The molecules initially excited into the first excited singlet state reach thermal equilibrium in a short time compared to the pumping time.

(c) Ground triplet to excited triplet state absorption is not negligible, but the population of the excited triplet state is negligible because of rapid nonradiative decay.

(d) The dye laser has essentially only three levels. (The fine vibrational and rotational levels in each main state are neglected.)

(e) The effect on state population densities caused by dye self-absorption of the lasing wavelength is negligible. (There are approximately two orders of magnitude difference between the absorption coefficient for the pumping wavelength and the expected lasing wavelength so this assumption is not too restrictive.)

(f) The point of maximum gain is reached so fast that the effect of reduction of the excited singlet state due to stimulated emission can be neglected. (This assumption has been shown to be realistic by Atkinson and Pace [34] and is very true at the onset of lasing; however, as lasing progresses and photon buildup occurs in the laser cavity the stimulated emission term can become very significant. The same is true of the self-absorption term since it also depends on intracavity power.)

Equations (9), (10A), (10B), and (10D) are used to evaluate the dye laser model in a computer simulation in Section IV. Equation (9), the gain equation, is used in the discussion of theoretical results to explain the theoretical time dependent wavelength sweep of the dye laser.

III. EXPERIMENTAL PROCEDURES AND RESULTS

A. EXPERIMENTAL SET UP

The apparatus used in generating and measuring the output of the Argon and dye lasers was set up as shown in Figure 3. A Beck Wavelength Reversion Spectroscope with a single line resolution of approximately four Angstroms was also used to monitor the dye laser output wavelength.

The beam splitter indicated in Figure 3 was actually an integral part of the front end of the Argon laser and is normally used as part of a power monitoring system. This system was modified so that the Argon laser output pulse could be monitored on an oscilloscope via a photodiode detector.

The diode detector and power meter were both tested for linearity and saturation at higher powers than could be expected at their locations in Figure 3. They both exhibited no signs of approaching saturation and their deviations from linearity over the testing range were minimal.

The risetime of the Argon laser is normally limited to seven nanoseconds because of cable transit times, etc., however, in the particular set up of Figure 3 the risetime was limited to 12 to 15 nanoseconds because that was the lower limit of the pulse generator risetime. An explanation of the cavity dump mechanism can be found in Maydan [35].

B. EXPERIMENTAL PROCEDURES

The first step in the procedure was the alignment of the Argon laser cavity dump system. This system consisted of a curved front half-mirror with vertical and horizontal adjustments, a rear curved mirror with vertical and horizontal plane tilt controls, and an acoustooptic cell housing

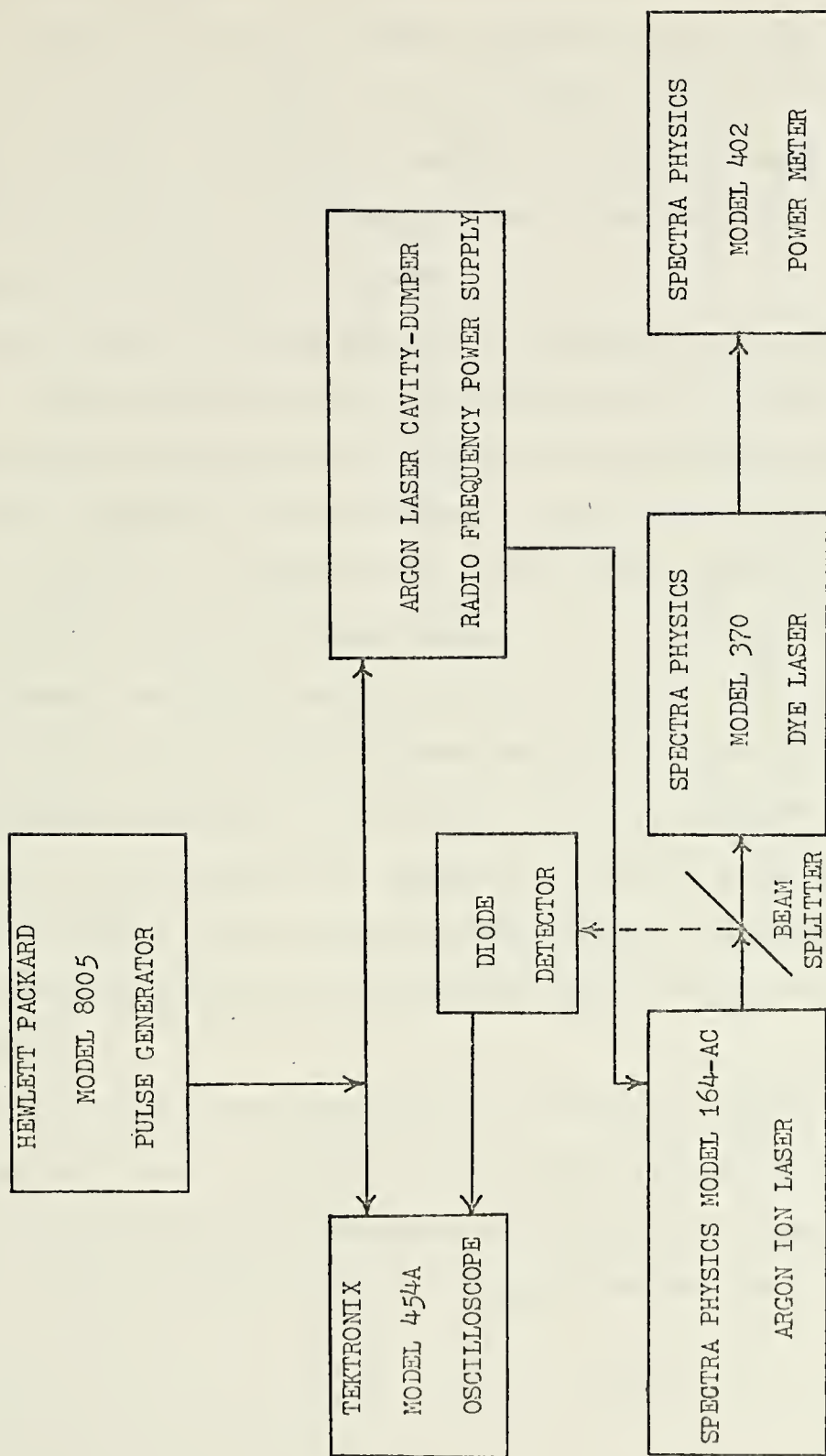


Figure 3: Experimental set up.

with controls to adjust its longitudinal and vertical positions as well as its angular alignment. All of these controls had to be precisely set for the cavity dump system to function properly, and the Argon laser power output and pulse shape had to be constantly monitored because some of the adjustments were extremely delicate. A slight movement of the rear mirror adjustments, for example, severely degraded the Argon laser output pulse and beam mode structure.

The next step in the procedure was the alignment of the Argon and dye lasers. This was done on a specially designed platform which had permanent hold down clamps for the Argon laser and kinematic mounts for the dye laser. Alignment of the two lasers was very sensitive and was a critical part of the experimentation since any nonparallelism of the dye and Argon laser cavities severely reduced the power conversion efficiency.

The Argon laser power supply was set for a current of 30 amperes after alignment was achieved. With the pulse generator delivering three volt, thirty nanosecond pulses at a repetition rate of one megahertz to the cavity-dump rf power supply, the average power output of the Argon laser was 500 milliwatts. These values and settings were then used as Argon laser operating reference points and standards for the rest of the experimentation.

The final step in the procedure was to monitor the output of the Argon and dye lasers. The Argon and dye laser powers were recorded, the Argon laser pulse shape was sketched, and the various dye laser wavelengths noted as the pulse width of the pulse generator was varied.

C. EXPERIMENTAL RESULTS

The results yielded some new and interesting properties of the dye laser. The wavelength of peak output power and efficiency of the cavity-dumped laser-pumped dye laser was found to occur at a shorter wavelength than that of the continuous wave laser-pumped dye laser. In addition, the tuning range of the pulsed dye laser was narrowed.

The normalized output for both the continuous-wave laser pumped and pulsed-laser pumped dye laser are shown for comparison in Figure 4. The same dye laser was used to obtain both curves.

A two piece mathematical model which is an excellent fit to the actual Argon laser output pulse used to obtain the pulsed dye laser curve is shown in Figure 5. The repetition rate of this pulse was one megahertz.

It was also discovered that as the pulse width driving the cavity-dumped rf power supply was lengthened the wavelength of peak emission shifted toward longer wavelength and the laser efficiency decreased. In addition, for a given pulse width, an increase in the output power of the Argon laser (accomplished by increasing the current to the Argon laser power supply) shifted the peak emission wavelength to shorter wavelengths.

The lowest peak wavelength observed was 5650 Angstroms and the highest conversion efficiency obtained was almost thirty percent. This same dye laser pumped with a continuous wave laser had an efficiency of only seventeen percent at the peak output wavelength of 5800 Angstroms.

The fluorescence spectrum of the dye in the laser was also measured by use of a spectroscope with a high intensity white light source. This spectrum along with the wavelength-power curve of the cavity-dumped laser-pumped dye laser are compared in Figure 6. It is obvious from this figure that the peak lasing wavelength for the pulsed pump is approaching the peak of the dye fluorescence curve.

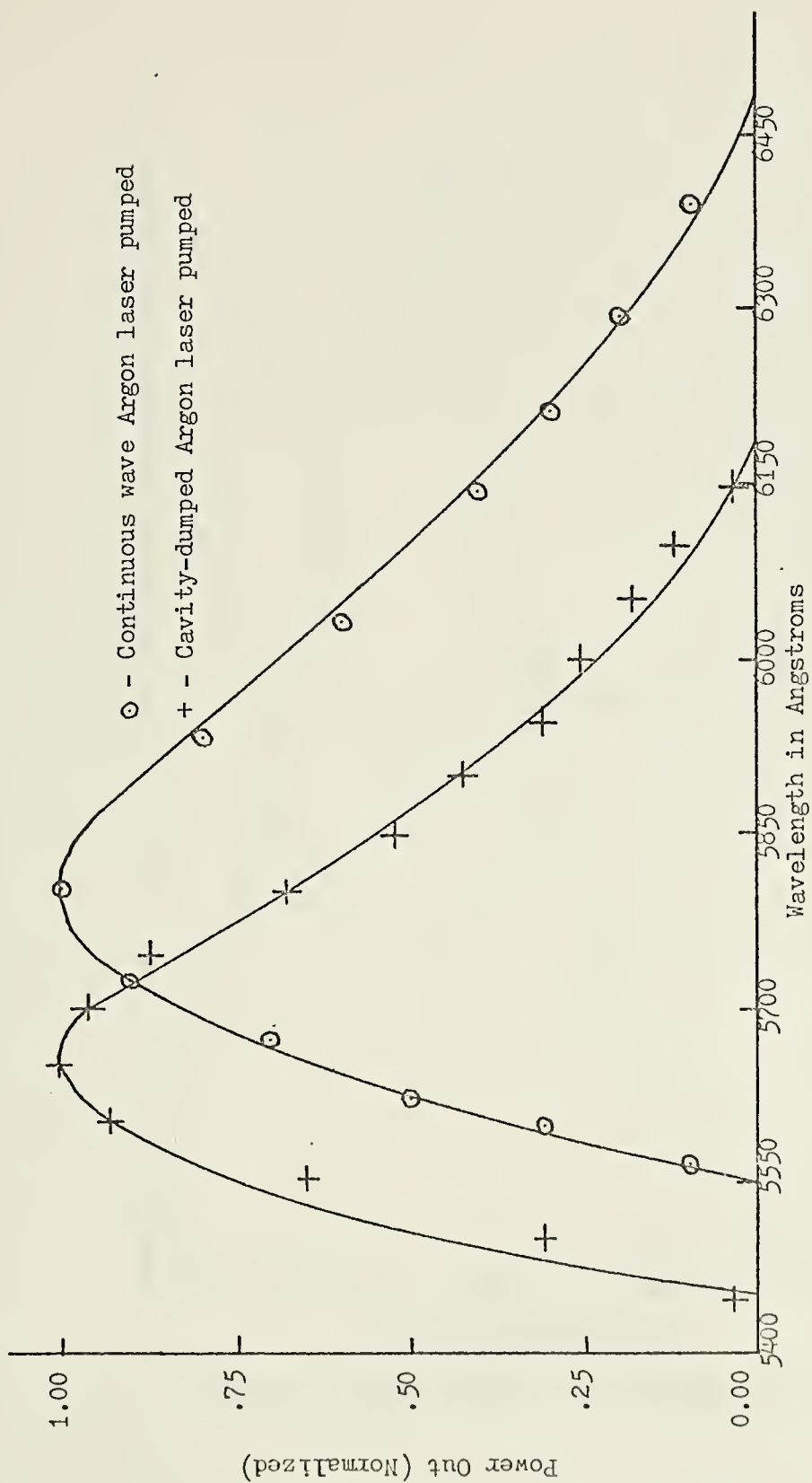


Figure 4: Power - wavelength spectra of a Rhodamine 6-G dye laser.

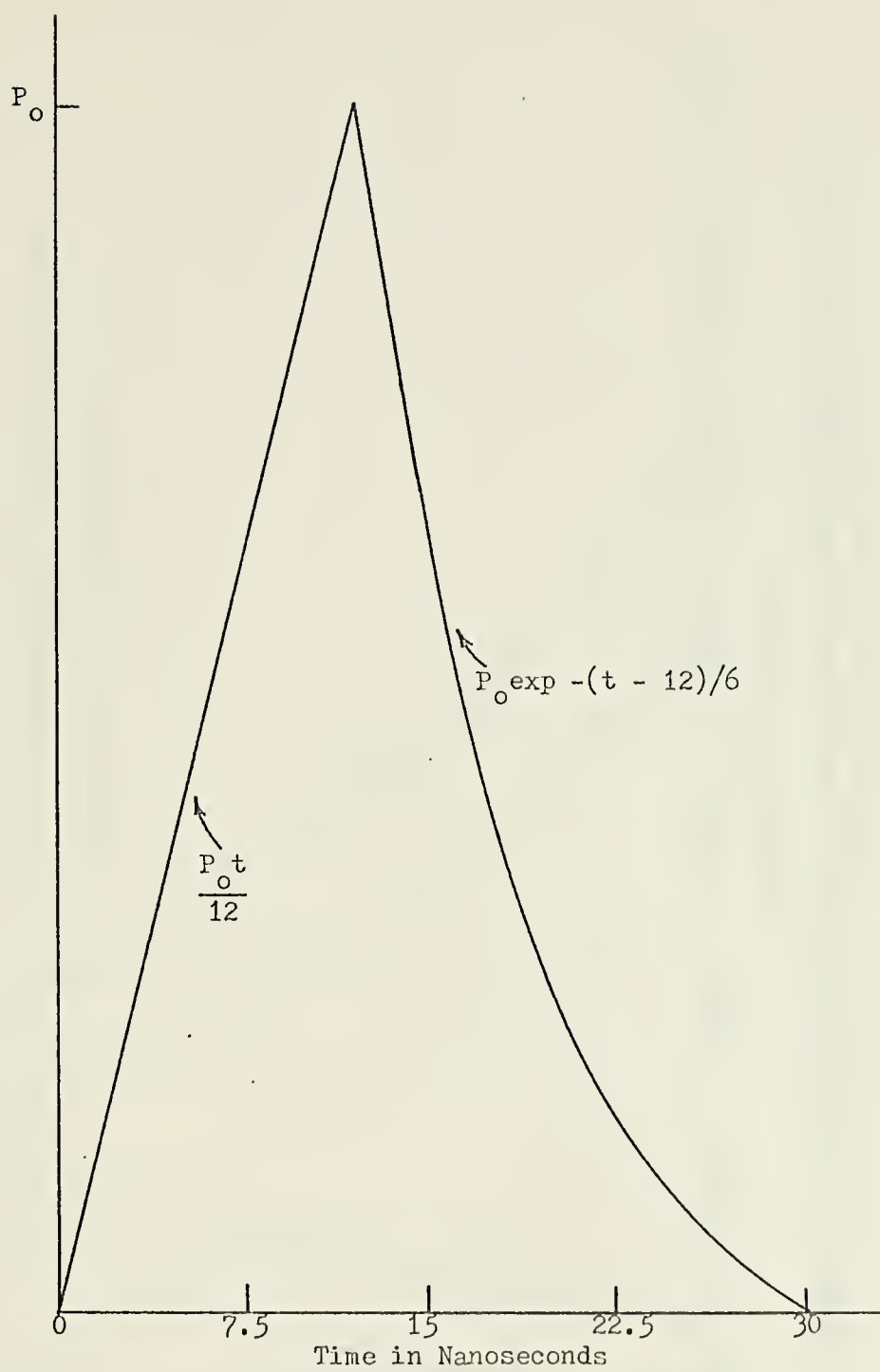


Figure 5: Typical Argon laser output pulse.

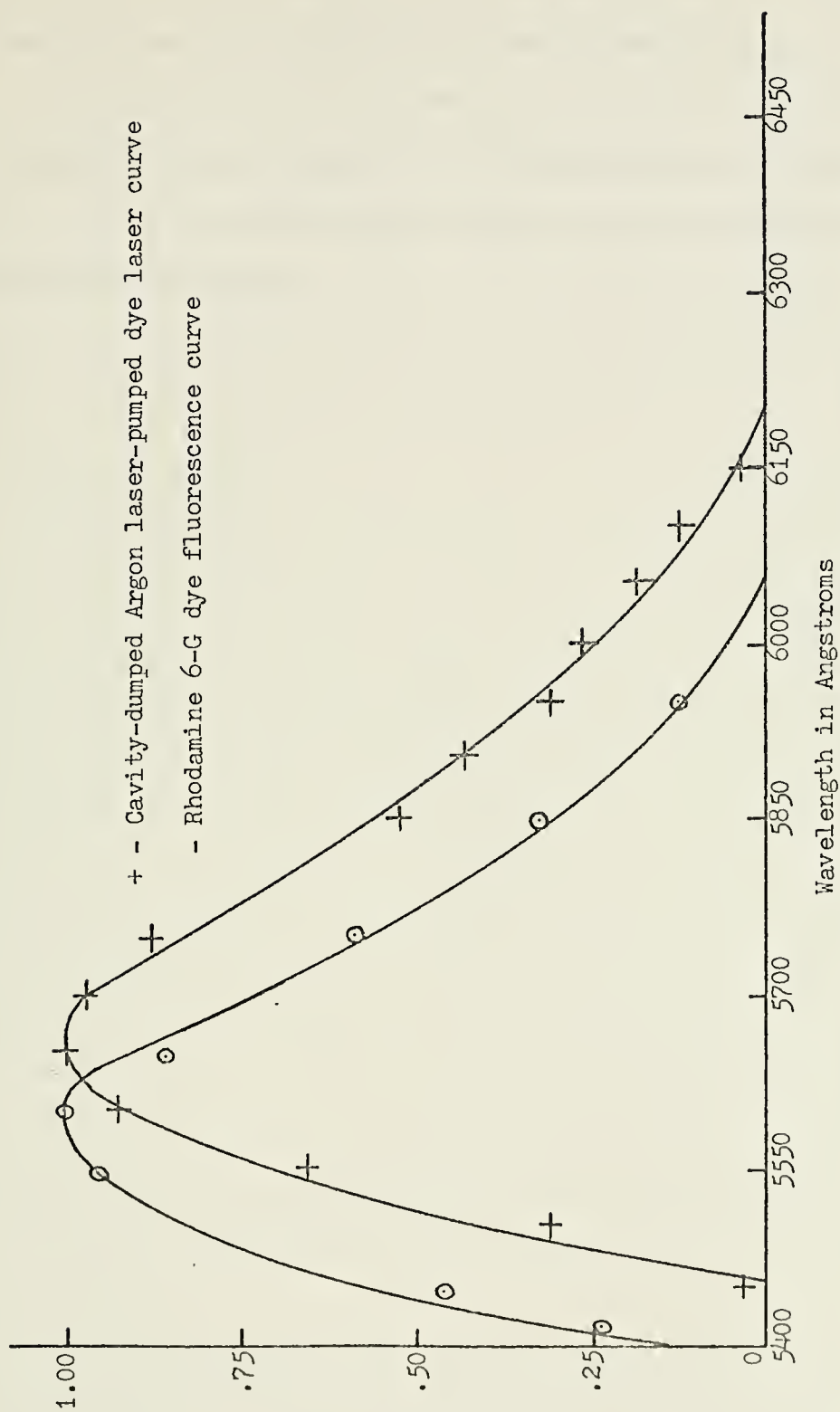


Figure 6: Wavelength-power curve of cavity-dumped Argon laser-pumped dye laser and Rhodamine 6-G fluorescence curve (Normalized).

A summary of the significant experimental observations is as follows:

(1) The pulsed dye laser wavelength spectrum exhibits a substantial green shift from the spectrum of the CW pumped dye laser.

(2) The shift increases and approaches the dye fluorescence curve as the pulse length from the cavity-dumper gets shorter.

(3) The efficiency is greater and the tuning range shorter for the pulsed dye laser.

IV. DYE LASER MODEL EVALUATION

Experimental results showed that the output wavelength spectrum of the cavity-dumped laser-pumped dye laser approached the dye fluorescence curve. The dye laser model of Figure 2 is analyzed in this section using equations (9), (10A), (10B) and (10D), which are the model gain and rate equations, and the pumping waveform of Figure 5 to determine if the spectrum shift can be predicted.

A. LITERATURE SURVEY

The first application of applying rate and gain equations to the dye laser was made by Sorokin, et al. [36, 22]. Their application assumed a Gaussian waveform pumping pulse and they attempted to predict the transient pulse shape of a pulsed Chloro-aluminum phthalocyanine (CAP) dye laser. They concluded from their results that a rapid pulse risetime was necessary or triplet state accumulation could prevent dye laser action.

The second analysis of Sorokin and his group again assumed a Gaussian pumping pulse and attempted to predict the efficiency of various dye lasers as functions of quantum efficiency and the excited singlet to triplet intersystem crossing rate constant (k_{st}). The results from this work yielded the prediction that dye laser efficiency should increase as the intersystem crossing rate time constant decreased or as the quantum efficiency increased.

A year later, in 1968, Bass, Deutsch and Weber [37] used the rate and gain equations to predict lasing frequencies and time to lasing for Gaussian shaped laser and flashlamp pumped dye lasers. They had

experimentally observed that a laser pumped dye laser emitted a shorter wavelength than when flashlamp-pumped, however, different laser cavities were used for the two pumping conditions and this led to different parameters entered in the gain equation and to the conclusion that differing cavity Q's accounted for the higher lasing wavelength of the flashlamp pumped case.

The following year Bass and Weber [38] again used dye laser rate and gain equations. This time they assumed a rather long Gaussian shaped pumping pulse and included triplet state effects in their discussions. They still concluded that cavity Q was the main determinant of lasing wavelength, however, they conceded that determination of lasing wavelength could be more complex if triplet state effects were significant.

In mid 1970 Keller [39] solved for pseudo steady state solutions to the rate equations (all time derivatives were set equal to zero) to investigate the effects of quenching agents on singlet and triplet state populations. He arrived at the conclusion that a specific quencher for the triplet state would markedly improve laser efficiency and that a substance that quenched both singlet and triplet states would usually improve the efficiency.

The next group to use rate equations was McColgin, et al. [33]. They considered triplet state effects but only under steady state conditions as is found in some continuous wave dye lasers, and they concluded that the emission wavelength adjusts itself so that the ratio of mirror losses, scattering losses, etc. to singlet absorption losses remains approximately constant.

Pappalardo, Samuelson and Lempicki [40] in 1972 used the rate equations to calculate the efficiency of dye lasers as a function of pump

parameters and triplet state lifetime for pump pulses in excess of one microsecond in duration. They assumed a Gaussian shaped pumping pulse and predicted that long pulse operation of up to 30 microseconds was feasible for short triplet state lifetimes but that the efficiency would go down as the pumping pulse was lengthened.

The most recent use of rate equations has been by Strome and Tuccio [17] who used results to improve their original dye laser [16], by Atkinson and Pace [34] who used them to calculate the lineshape of a Fabry-Perot etalon tuned Rhodamine 6-G dye laser, and by Streifer and Saltz [41] who used the equations to analyze an acoustooptically tuned dyelaser.

B. GAIN AND RATE EQUATION PARAMETERS

The evaluation of the dye laser system rate and gain equations for a cavity such as the one in Figure 2 requires a lot of physical data. The actual dye used to obtain the experimental data had a mixture of methanol and water as the dye solvent; however, there is no information available on the dye in this particular solvent hence physical data available for ethanol solutions was used. It was assumed that any predictions or conclusions based on the results would apply to Rhodamine 6-G in the actual solvent. (The main difference in the solvents is that both the singlet absorption and fluorescence spectrum peaks are further in the green region of the visible spectrum when the solvent is 100 percent ethanol.)

The fluorescence lineshape and singlet absorption cross section of a 10^{-4} Molar solution of Rhodamine 6-G in ethanol are shown in Figure 7. These curves were obtained by F. Grum of Kodak Research Laboratories and were reproduced in Reference 8. Snavely [8] measured the fluorescence yield of the dye and obtained a value of $\phi = 0.83$ and the fluorescence spectrum of Figure 7 is normalized to this value; i.e.

$$\int_{-\infty}^{\infty} E(\lambda) d\lambda = \phi = 0.83.$$

There is no data available on the triplet absorption cross section for an alcohol solution of Rhodamine 6-G. The only available curve is shown in Figure 8 which was determined by Buettner [42] using a flash photolysis technique for Rhodamine 6-G in polymethyl methacrylate.

Several values of singlet and triplet state lifetimes are given in the literature. The various values given for T_s are 7.4 nsec in Weber and Bass [38], 4.8 nsec in McColgin, et al. [33], 7.3 nsec in Snively and Peterson [31], and 5.5 nsec in Mack [43]. The reason for the use of different values by the groups mentioned above is due to different measured values. An average value of 6.3 nsec was used in this analysis because there were no significant reasons why one value should be preferred.

There are also many values of T_t given in the literature, but the best evidence available suggests that the most reasonable value is 100 nsec. Keller [39] arrived at this value in his analysis of Oxygen quenching in an alcohol solution and Snively and Schafer [9] obtained 100 nsec as a measured value.

The value of the intersystem crossing rate constant, k_{st} , can be determined from the formula

$$k_{st}^{-1} = T_s \phi / (1 - \phi) \quad (11)$$

which is found in Snively [8] and others. The value of 0.84 from Bass and Steinfeld [44] is the most common value found for ϕ and since the value of 6.3 nsec is assumed for T_s , (11) yields the value of 29.4 nsec for k_{st}^{-1} . The fluorescence spectrum of Figure 7 is normalized using $\phi = 0.83$ so that spectrum and equation (11) are compatible.

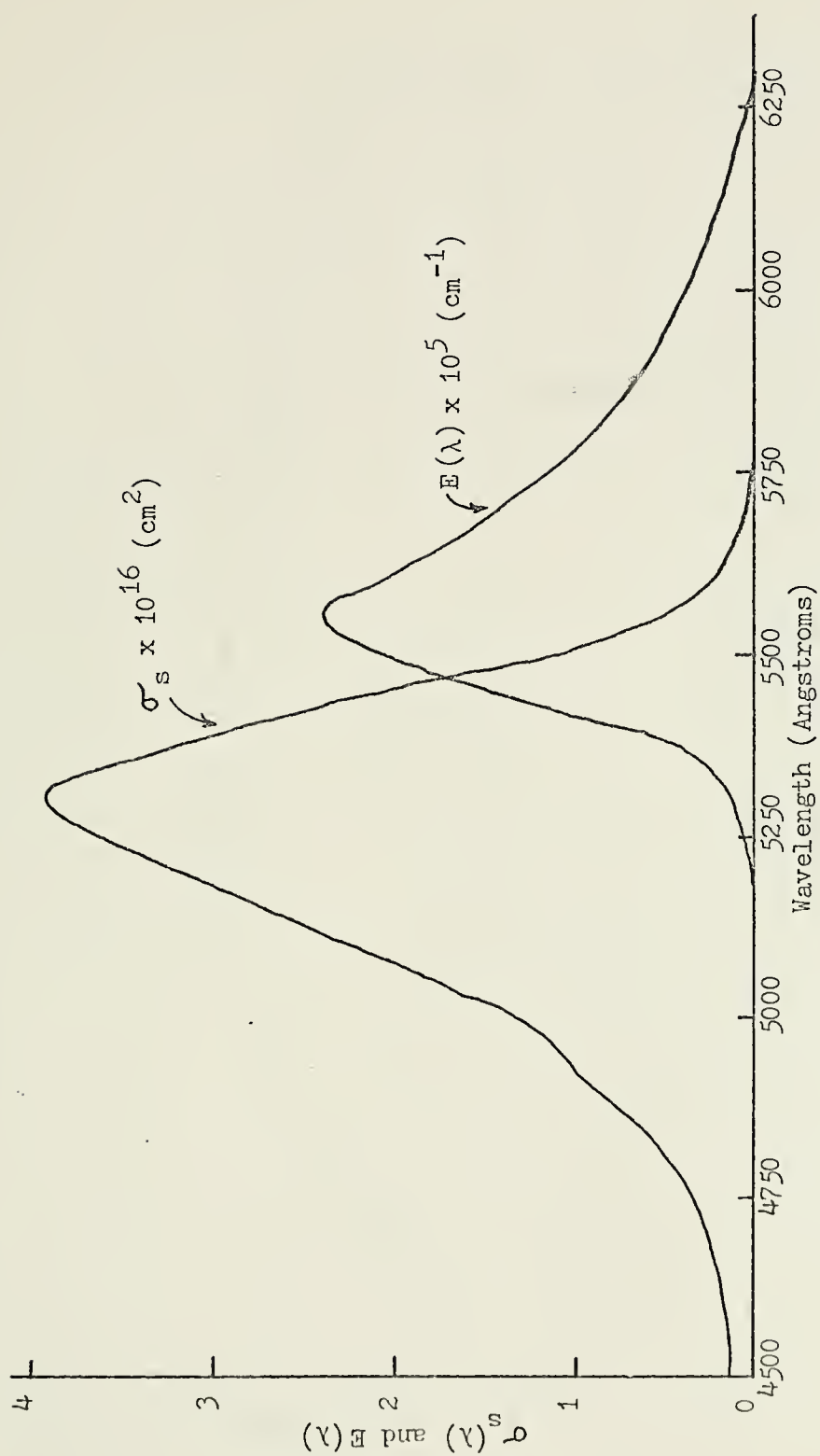


Figure 7: Singlet state absorption cross section and fluorescence spectrum of 10^{-4} Molar Rhodamine 6-G in ethanol [8].



Figure 8: Triplet state absorption coefficient of Rhodamine 6-G in polymethyl methacrylate [42].

The easiest constant to evaluate is N, the total molecular density. The actual dye solution was 3×10^{-4} Molar so that

$$N = 3 \times 10^{-4} \text{ Molar} \times \frac{1 \text{ gram-mole}}{1 \text{ Molar-liter}} \times \frac{6.023 \times 10^{23} \text{ molecules}}{\text{gram-mole}} \times \frac{1 \text{ liter}}{10^3 \text{ cm}^3}$$

which is 1.8×10^{17} molecules/cm³. This assumes that the density of the solvent at room temperature is approximately the same as at the standard reference temperature.

The values of $L_1 = .1$ cm, $R_1 = .995$ and the curve of R_2 versus wavelength were obtained from the manufacturer [45]. The dye cell windows were anti-reflection (AR) coated so typical values for AR surfaces of .98 were used for T_1 and T_2 .

The remaining constants needed for evaluation of $\sigma_e(\lambda)$ are c, the speed of light, and \bar{n} , the index of refraction. The value used for the speed of light was 3×10^{10} centimeters/sec and the index of refraction of the dye solution was approximately 1.33.

The optical pumping rate, $P(t)$, may be written as $\sigma_p I_p / hf_p$ where σ_p is the dye absorption cross section for f_p , the pump frequency, h is Plancks constant and I_p is the pump irradiance in watts/cm². The pump wavelength was 5145 Angstroms and the corresponding frequency was 5.82×10^{14} sec⁻¹. Plancks constant has a value of 6.625×10^{-34} sec⁻¹. The value of 2.37×10^{-16} cm² obtained from Figure 7 was used for σ_p .

Pump irradiance can be written as power per unit area. The model of the pump power as a function of time is shown in Figure 5. The average power output of the Argon laser was 0.5 watts and the value of 42.7 watts for P_0 was obtained from the formula

$$P_{\text{average}} = \frac{1}{T} \int_0^T P(t) dt.$$

There is a problem in defining the effective area and volume in which the pump beam is absorbed. Jacobs, Samuelson, and Lempicki [46] assumed uniform pumping in their analysis of losses in a continuous wave dye laser and used the beam waist area as the effective pumped area. At least some of the Argon laser beam must exit the dye volume before uniform pumping can be assumed [40], otherwise the amount of beam penetration into the dye and the size of the pumped volume cannot be determined. The dye laser used in the experiment allowed approximately five percent of pump power to exit the dye cell [45], therefore, uniform pumping was assumed. The beam waist radius was six microns [45] so the assumed effective area was $1.13 \times 10^{-6} \text{ cm}^2$.

The assumption of uniform pumping is one of the most marginal in dye laser analysis. The complexities introduced by trying to evaluate mode-matching of the pump and dye laser beams in the dye cell and nonuniform excitation of dye molecules, however, makes the assumption practical.

C. GAIN AND RATE EQUATION SOLUTIONS

1. Solution Method

The first step in the theoretical analysis was the solution of the rate equations for the state population densities as a function of time. The solution was carried out using a program entitled INTEGL of the U.S. Naval Postgraduate School Computer Library. (See Appendix A) INTEGL uses a fourth order Runge-Kutta method with programmable step size changes to achieve the solution to simultaneous ordinary differential equations. The only modifications made to the INTEGL program were those necessary to enable it to handle the wide range of parameter values used in the rate equations.

The values of the state population densities were then used to evaluate the gain equation. This was accomplished by first selecting values of state densities at a particular time and then evaluating the gain using the wavelength dependent parameters over a large range of wavelengths. The succeeding steps followed the same pattern and this was continued until the point of maximum gain versus time and wavelength reached a constant relationship; i.e., the wavelength of maximum gain remained unchanged with time.

The purpose of evaluating the gain in this manner was that the lasing wavelength of the laser model should be where the gain is maximum. This was then compared to the dye fluorescence spectrum to see where the lasing wavelength was in relation to the peak wavelength of the spectrum.

The last step was to predict where the experimental laser should lase based on the theoretical comparison and the fluorescence spectrum of the experimental dye. Theoretical and experimental results should agree if theory was sound.

2. Theoretical Results

A graph of the peak gain wavelength versus time is shown in Figure 9. It can be seen from the figure that lasing starts at the longer wavelengths and sweeps toward the shorter wavelengths. Figure 9 also contains a graph of the ratio of triplet state population to ground singlet state population (N_t/N_o) versus time.

The results of evaluation of the gain versus wavelength at steady state is shown in Figure 10. It can be seen that the peak wavelength (5570 Angstroms) corresponds to the peak wavelength of the Rhodamine 6-G fluorescence curve of Figure 7.

The results displayed in Figure 9 and the gain equation, equation (9) of Section II, can be used to explain the theoretically obtained dye

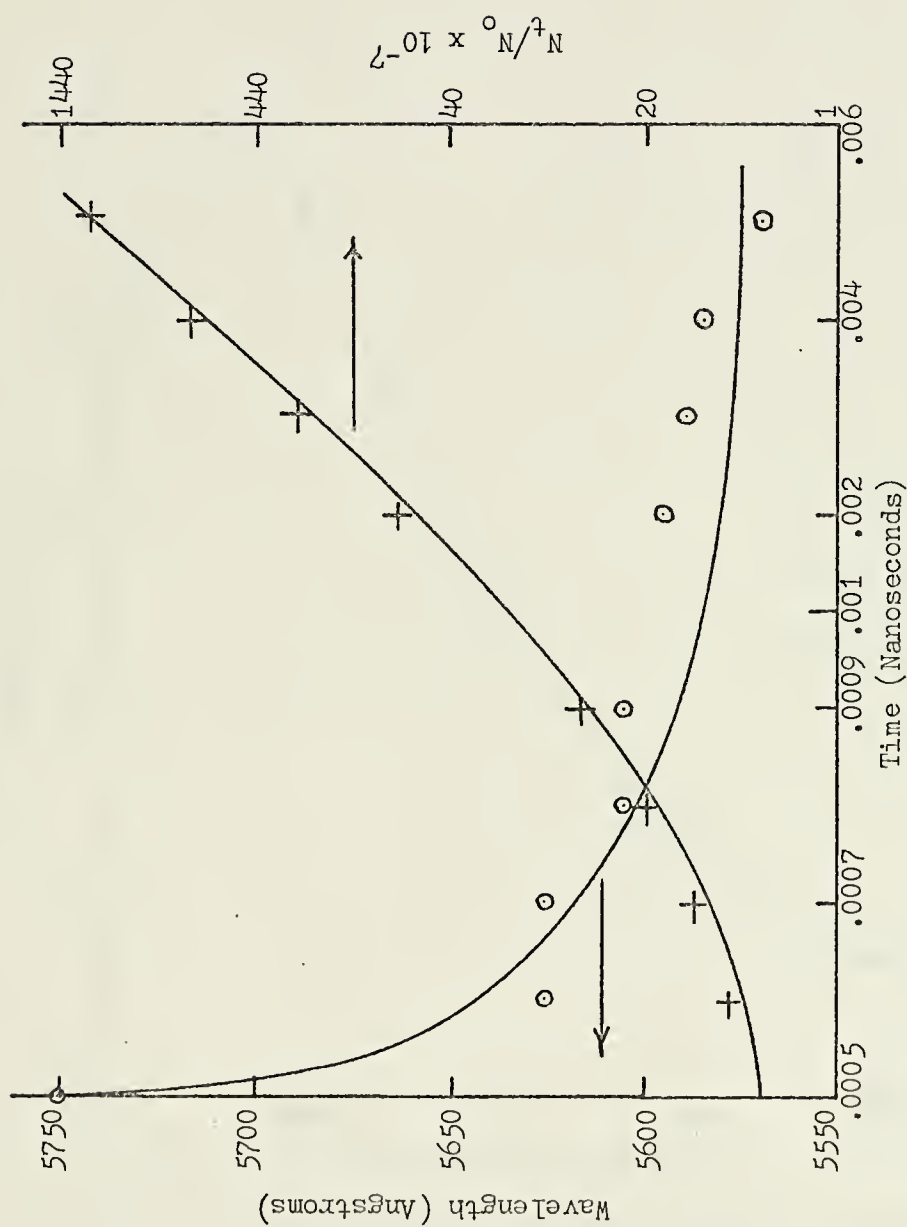


Figure 9: Peak gain wavelength and ratio of triplet to ground singlet state population for 3×10^{-4} Molar Rhodamine 6-G laser model.

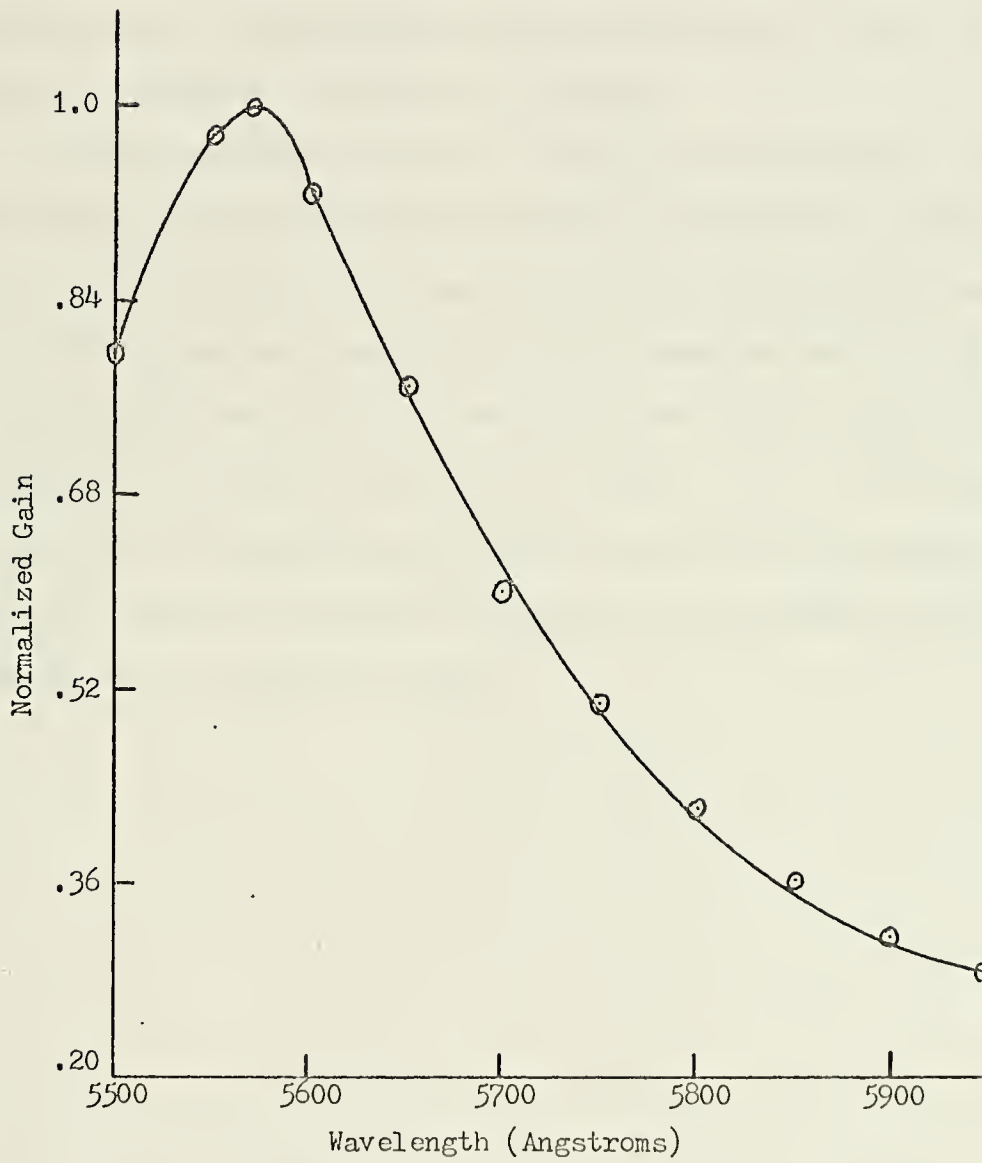


Figure 10: Theoretical normalized gain versus wavelength for Rhodamine 6-G dye laser model.

laser wavelength sweep. The two wavelength dependent losses in the gain equation are caused by singlet and triplet absorption. The ratio of N_t/N_o at the onset of lasing is very small indicating domination of the singlet state absorption loss. (Singlet absorption is associated with N_o and triplet absorption with N_t .) Figure 7 shows that singlet absorption is greatest for shorter wavelengths, hence there should be a tendency for long lasing wavelengths at the onset of lasing.

As pumping continues the ratio of N_t/N_o becomes greater. This indicates that as time passes there should be a tendency for triplet absorption losses to dominate. Figure 8 shows that triplet absorption is greater at the longer wavelengths (up to 6000 Angstroms which is within the lasing range of Rhodamine 6-G) and, therefore, the dye laser should end up lasing at wavelengths closer to the peak of the dye fluorescence curve. (The above statements are true in this case for the specific pulse model of Figure 5. Pulses of different shape, duration, and intensity may or may not cause the sweep.)

V. CONCLUSIONS

A. EXPERIMENTAL AND THEORETICAL COMPARISON

The theoretical analysis predicted that for the pumping pulse model of Figure 5 and after a wavelength sweep of very short duration the dye laser would lase at or near the peak of the dye fluorescence spectrum. It was observed experimentally that the dye laser lased approximately 50 Angstroms from the peak of the dye fluorescence curve in the pulsed case (Figure 6) rather than 200 Angstroms as in the continuous wave pumped case (Figures 4 and 6). It may be concluded, therefore, that theory and experimentation are in agreement within the limits of the assumptions made in the study.

The variable of least confidence in the entire analysis was the experimental dye fluorescence curve. The peak of the fluorescence curve for Rhodamine 6-G in an ethanol solution is typically about 5570 Angstroms [8] and in a water solution is about 5750 Angstroms [46]. The actual solvent was determined by nuclear magnetic resonance measurements to be approximately two-thirds water and one-third methanol. This should have caused the fluorescence peak of the dye to be somewhere around 5660 to 5700 Angstroms which is much closer to the observed peak wavelength than the 5600 Angstrom peak of the fluorescence curve of Figure 6. One explanation for the difference between the measured and expected fluorescence peaks is the fact that the spectrometer calibration curve used to measure the experimental dye fluorescence spectrum had a steep slope and was very sensitive to spectrometer dial readings.

B. REMARKS

The decrease in efficiency of the dye laser as the pulse length was widened can be explained very simply in terms of the rate equations. The lengthening of the pulse decreased the peak power of the pumping pulse which in turn caused a longer time to reach the onset of lasing. As a result, the triplet state had more time to build up and extract molecules from the singlet lasing system - efficiency had to decrease. There are several things which hinder the analysis of the dye laser. There is not much data available on dye properties in various solvents and the properties of the triplet state are still pretty much unknown. There is also a lot to be learned about the effects of thermal heating and nonuniform pumping of the dye and no one as yet has begun to investigate the effect of chemical reaction and relaxation rates on the dye laser. Stability and noise considerations also require investigation.

APPENDIX A

DYE LASER RATE EQUATION COMPUTER PROGRAM LISTING

The computer listing on the following pages contains the program for the solution of the dye laser rate equations. The main part of the program is SUBROUTINE INTEG1 and the comments preceding its operational statements completely describe its use. The rate equations in the program correspond to equations (10A), (10B) and (10D) of Section II. The data cards used in the actual solution and described in the usage comments of INTEG1 are located at the end of the listing.

INTEG1 had to be modified to some extent so it could handle a wider range of parameter values than was originally allowed. These modifications included input and output format and an increase in the number of allowed integration steps and pages of output, but no changes were made to the basic fourth order Runge-Kutta integration and other computational algorithms.

DYE LASER RATE EQUATION SOLUTION

```

//SNY92C83 JOB (2083,029C,DC12),'SNYDER, G. W.',TIME=2
// EXEC FORCLG,REGION=GC=100K
//FCRT .SYSDD *
DIMENSION X(30),XDCT(30),C(15)
C(10)=1.0
1 CALL INTEG4(T,X,XDCT,C)
IF(T.GE.0.001) GO TO 2
C(11)=1.0C
C(12)=1.0C
GO TO 3
2 C(11)=1
C(12)=1
IF(T.LE.0.1) GO TO 3
C(11)=1.0C
C(12)=1.0C
3 CONTINUE
Y = POWER(T)

```

CCCCCCCC

THE THREE EQUATIONS BELOW ARE THE DYE LASER RATE EQUATIONS AND
 CORRESPOND TO EQUATIONS 10A, 10B AND 10D OF SECTION III. IN THE
 EQUATIONS X(1) IS THE EXCITED SINGLET STATE POPULATION, X(2) IS THE
 TRIPLET STATE POPULATION AND X(3) IS THE GROUND SINGLET STATE POPULATION.

```

XDCT(1) = -C(2)*X(1) + C(6)*C(3)*C(7)*C(7)*Y - .542*Y*X(1) -
1.542*Y*X(2)
XDCT(2) = - C(4)*X(2) + C(5)*X(1)
X(3) = 18.0*C(7)*C(7)*C(7) - X(1) -X(2)
GO TO 1
END

```

CCCC

FUNCTION POWER (Z) BELOW IS THE ARGON LASER POWER AS A FUNCTION OF
 TIME IN ACCORDANCE WITH THE TWO SEGMENT CURVE OF FIGURE 5.

```

FUNCTION PCWER(Z)
IF(Z.GE.12.0) GO TO 10
PCWER = (42.7*Z)/12.0
1C PCWER = 42.7*EXP((12.0-Z)/6.0)
RETURN
END

```


EQUATION STATEMENTS

THE NUMBER OF EQUATIONS TO BE SOLVED, "N", MUST BE LESS THAN THE NUMBER 30. THEY MUST BE REDUCED TO ACCORD WITH SUBSCRIPTED EQUAL 30. THEN EXPRESSED IN FCRTAN. STANDARD NON SUBSCRIPTED FORM AND MAY BE USED AS WELL AS STANDARD LIBRARY FUNCTIONS. VARIABLES MAY BE USED IN THE ORDER OF THE EQUATIONS IS USUALLY VARIOUS. A TYPICAL SET MIGHT READ:

```
ERROR= SIN(C(1)*T)-X(1)
XDOT(1)=X(2)-.1*X(1)
XDOT(2)=ERROR+C(2)*XDOT(1)
```

THE X ARRAY CONTAINS THE DEPENDENT VARIABLES. THE XCCT ARRAY CONTAINS THE FIRST DERIVATIVE WITH RESPECT TO THE INDEPENDENT VARIABLE ("T" IN THIS EXAMPLE). THE REGRESSION TC BE SUPPLIED BY THE USER. EACH "XCCT" IN TERMS OF THE VALUES IN THE AND DEPENDENT VARIABLES, CONSTANTS IN THE XCCT ARRAY.

```

CONSTANTS (C(1), ILE=8) ARE READ FROM A DATA CARD. CCNSTANT
CC(10) MUST NEVER BE USED EXCEPT AS IN THE SAMPLE SETUP CF
ABOVE. C(1), C(12), AND C(13) CONTROL FREQUENCY OF
INTEGRATION; C(12) IS THE SIZE OF THE STEP IN STATE-
THE DEFAULTS ARE PRINTED EVERY STEP AND PLotted BY STATE-
GENERATED ON EACH INTEGRATION. C(13) MAY BE CHANGED TO "STATE-
DEFINING THEM BETTER. THESE "CALL THE SOLUTION" SUCH AS:

```

$$\begin{aligned} C(11) &= 10. \\ C(12) &= 1. \end{aligned}$$

CAUSES PRINT-CUT TO TAKE PLACE AT EVERY 10 STEPS AND PLOT
POINTS TO BE GENERATED AT EACH STEP. NOTE THAT NO MORE THAN
4500 INTEGRATION STEPS, 450 LINES OF PRINT-OUT, OR 900 PLOT
POINTS CAN BE GENERATED IN ANY ONE RUN.

ANY LEGAL FORTRAN STATEMENT OR TECHNIQUE CAN BE USED IN THE CALLING PROGRAM, PROVIDED THAT A TRANSFER OF CONTROL OCCURS EACH STEP OF THE PROCESSING OF ALL RELEVANT STATEMENTS DURING EACH STEP OF THE INTEGRATION. FOR EXAMPLE THE FOLLOWING WOULD BE ALLOWED:

```

3 2
IF(T-10.0) 3,2,2
C(1)=0.
2 CONTINUE

```


INT1109560
INT1109570
INT1109580
INT1109590
INT1109600
INT1110100
INT1110200
INT1110300
INT1110400
INT1110500
INT1110600
INT1110700
INT1110800
INT1110900
INT1111000
INT1111100
INT1111200
INT1111300
INT1111400
INT1111500
INT1111600
INT1111700
INT1111800
INT1111900
INT1112000
INT1112100
INT1112200
INT1112300
INT1112400
INT1112500
INT1112600
INT1112700
INT1112800
INT1112900
INT1113000
INT1113100
INT1113200
INT1113300
INT1113400
INT1113500
INT1113600
INT1113700
INT1113800
INT1113900
INT1114000
INT1114100
INT1114200
INT1114300

WHICH CAUSES C(1) TO TAKE THE VALUE SPECIFIED CN THE DATA CARD
FOR T.LT.10. AND THE VALUE 0. FOR T.GE.10. ONLY. QUANTITIES
X(I) AND T CAN BE OUTPUT. IF SOME QUANTITY OTHER THAN THE
INDEPENDENT VARIABLE, DEPENDENT VARIABLE OR DERIVATIVE
IS DESIRED AS OUTPUT, IT MUST BE EQUATED TO AN X(I) SUCH THAT
N.LT.1.LE.30. SUCH AS:

X(3)=ERRCR
X(4)=ERRCR*ERROR.

ALL SUCH AUXILIARY EQUATIONS MUST BE PLACED BETWEEN THE
"CALL INTEG1" AND "GO TO 1" STATEMENTS.

DATA CARDS

FIRST: CONTAINS A JOB IDENTIFICATION LABEL PUNCHED IN CCLS 1 TO
48. IT WILL BE REPRODUCED IN THE PRINT-OUT.

SECOND: CONTAINS THE NUMBER OF RUNS TO BE PROCESSED (.LE.9)
PUNCHED IN COL 1. THE RUN NUMBER IS PLACED ON ALL OUTPUT
ALONG WITH THE ABOVE JOB IDENTIFICATION.

THIRD: CONTAINS THE VALUE OF N, THE NUMBER OF EQUATIONS TO BE
SOLVED. PUNCHED RIGHT-JUSTIFIED IN CCLS 1 AND 2.
WHEN N IS LESS THAN 10, IT MUST BE PUNCHED IN COL 2.
WHEN IT IS EQUAL TO OR GREATER THAN 10, IT MUST BE PUNCH-
ED IN CCLS 1 AND 2. IT MUST BE LESS THAN OR EQUAL TO 30.

FOURTH: INTRODUCES THE INITIAL AND FINAL TIMES CF T (TI & TF)
TOGETHER WITH THE STEP-SIZE(S), CT. THE INTEGRATION CAN
BE PROCESSED IN UP TO 3 SEGMENTS, EACH WITH A DIFFERENT
STEP-SIZE, THUS THE DATA CARD CAN CONTAIN:

TI - CT1 - TF
TI - DT1 - TF1 - CT2 - TF2 - CT3 - TF
OR TI - CT1 - TF1 - CT2 - TF2 - CT3 - TF

THE CORRESPONDING DATA VALUES ARE PUNCHED (WITH DECI-
MALS), IN THE ABOVE ORDER, IN CCLS 1-10, 11-20, 21-30,
...61-70.

FIFTH: CONTAINS THE CONSTANTS C(1) THRU C(8) PUNCHED (WITH
DECIMALS) IN CCLS 1-10, 11-20, ...71-80. BLANK MAY BE
USED FOR EITHER ZERO OR UNUSED CONSTANTS.

SIXTH: CONTAINS THE INITIAL CONDITIONS (X(1)(0)) THROUGH
(X(N)(0)) IN THE SAME FORMAT AS THE FIFTH CARD. ADDI-


```

5000 FCRMAT(2F15.6)
      TF = TF1
      IF(DT2.NE.0.) GO TO 9
      WRITE(6,206) I, TF
206 FCRMAT (22H INITIAL TIME
      = ,E19.11, /
      = ,E19.11)
207 FCRMAT (22H FINAL TIME
      = ,E19.11)
      WRITE(6,207) DT
      FCRMAT (22H STEP SIZE
      = ,E19.11)
      GO TO 12
      IF(DT3.NE.0.) GO TO 11
      TF = TF2
      WRITE(6,206) I, TF
      WRITE(6,208) DT, I, TF1, DT2, TF1, TF2, DT3, TF
208 FCRMAT (22H STEP SIZE
      = ,E19.11, 13+ BETWEEN T = ,E19.11,
      9H AND T = ,E19.11)
      GO TO 12
      TF = TF3
      WRITE(6,208) DT, I, TF1, DT2, TF1, TF2, DT3, TF
11 FCRMAT (5,5001) (C(I), I=1,8)
12 FCRMAT (8F10.4)
5001 FCRMAT (5,106) (X(I), I=1,NN)
106 FCRMAT (3F25.5)
      J = 0
      DO 14 I=1,8
      IF(C(I).NE.0.) J=J+1
      CCNTINUE
14 K = 0
      DO 16 I=1,NN
      IF(X(I).NE.0.) K=K+1
      CCNTINUE
16 IF(J - 1) 17,18,19
17 WRITE (6,209)
209 FCRMAT (/ ,34H ALL THE CCNstants, C(I), ARE ZERO )
18 FCRMAT (6,210)
210 FCRMAT (/ ,30H THE ONLY NON-ZERO CCNstant IS )
      GO TO 423
19 WRITE (6,211)
      FCRMAT (6,211)
      FCRMAT (/ ,35H THE NON-ZERO CCNstants, C(I), ARE )
211 FCRMAT (6,211)
420 FCRMAT (6,211)
      FCRMAT (/ ,35H THE NON-ZERO CCNstants, C(I), ARE )
      FCRMAT (6,211)
      FCRMAT (/ ,35H THE NON-ZERO CCNstants, C(I), ARE )
212 FCRMAT (6,211)
422 FCRMAT (6,211)
      FCRMAT (/ ,35H THE NON-ZERO CCNstants, C(I), ARE )
      FCRMAT (6,211)
      FCRMAT (/ ,35H THE NON-ZERO CCNstants, C(I), ARE )
423 FCRMAT (6,211)
      FCRMAT (/ ,35H THE NON-ZERO CCNstants, C(I), ARE )
424 FCRMAT (6,211)
      FCRMAT (/ ,35H THE NON-ZERO CCNstants, C(I), ARE )
1209 FCRMAT (6,211)
      FCRMAT (/ ,35H THE NON-ZERO CCNstants, C(I), ARE )
425 FCRMAT (6,211)
      FCRMAT (/ ,35H THE NON-ZERO CCNstants, C(I), ARE )

```

INT12390
INT12400
INT12410

INT12440
INT12460
INT12470
INT12480
INT12490
INT12500

INT12530
INT12540
INT12550

INT12580
INT12590
INT12600
INT12610
INT12620
INT12630
INT12640
INT12650
INT12660
INT12670
INT12680
INT12690
INT12700
INT12710
INT12720
INT12730
INT12740
INT12750
INT12760

INT12780
INT12790
INT12800
INT12810
INT12820
INT12830


```

1210 FCRMAT (/ , 39H THE ONLY NON-ZERO INITIAL CCNCITION IS )
      GC TO 427
426 WRITE (6, 1211)
1211 FCRMAT (/ , 36H THE NON-ZERO INITIAL CONDITIONS ARE )
427 CC 429 I=1, NN
      IF (X(I).NE.0.) WRITE(6, 1212) I, X(I)
1212 FCRMAT (14X, 2HX( , 12, 4H) = , E25.5)
429 CCNTINUE
      READ (5, 104) (JTITLE(I), IP(I), I=1, 8)
104 FCRMAT(8(A8, I2))

C CHECK FOR THE NUMBER OF COLUMNS CALLED FOR BY LOCATING FIRST
C BLANK COLUMN HEADING
C
CC 21 J=1, 8
      IF (JTITLE(J).EQ. IBLANK) GO TO 22
21 CCNTINUE
      JJ = J - 1
22 JJ = J - 1

C JJ IS NOW THE NUMBER OF COLUMNS. REPEAT WITH THE GRAPHS.
C
C
105 READ (5, 105) (KTITLE(I), KTITLE(I+1), IG(I), IG(I+1), I=1, 7, 2)
      FCRMAT (4(2A8, 2I2))
CC 24 K=1, 7, 2
      IF (KTITLE(K).EQ. IBLANK.AND. KTITLE(K+1).EQ. IBLANK) GC TO 25
24 CCNTINUE
      KK = K/2
      KK*2 = K
      MULTIP = KK*2
      IF (KK.NE.1) GO TO 306
      IF (IG(3).EQ.0) GO TO 306
      IF (IG(5) + IG(6).NE.0) GO TO 303
      MULTIP = 2
      KKK = 4
      GC TO 306
      IF (IG(7) + IG(8).NE.0) GO TO 305
303 MULTIP = 3
      KKK = 6
      GC TO 306
      MULTIP = 4
      KKK = 8
305 MULTIP = 8

C IF MULTIP = 0, KK IS THE NUMBER OF SINGLE CURVE GRAPHS. OTHERWISE
C MULTIP IS THE NUMBER OF CURVES ON A SINGLE GRAPH.
C
306 IF (JJ.EQ.0) GO TO 27

```

INT112840
INT112850
INT112860
INT112870
INT112880
INT112890
INT112900
INT112910

INT112940
INT112950
INT112960
INT112970
INT112980
INT112990
INT113000
INT113010
INT113020
INT113030
INT113040
INT113050
INT113060
INT113070
INT113080
INT113090
INT113100
INT113110
INT113120
INT113130
INT113140
INT113150
INT113160
INT113170
INT113180
INT113190
INT113200
INT113210
INT113220
INT113230
INT113240
INT113250
INT113260
INT113270
INT113280
INT113290
INT113300
INT113310


```

214 WRITE(6,214) (JTITLE(1),IP(1),I=1,JJ)
      FCRMAT (///,56H THE COLUMN HEADINGS AND THE CRRRESPONDING VARIABLES
      IS ARE ,//,(15X,A8,9X,2HX(,12,1H)))
      GC TO 28
215 WRITE(6,215)
      FCRMAT (///,25H NO PRINTOUT IS REQUIRED )
216 IF(KK.EG.0) GC TO 308
217 IF(MULTIP.NE.0) GC TO 309
      IF(KK.NE.1) GC TO 307
218 WRITE(6,216) KTTITLE(1),KTTITLE(2),IG(1),IG(2)
      FCRMAT (///,52H THE GRAPH TITLE AND THE CRRRESPONDING VARIABLES AR
      LE ,//,10X,2A8,4X,2FX(,12,8H) VS. X(,12,1H))
      GC TO 31
219 WRITE(6,217) (KTTITLE(1),KTTITLE(1+1),IG(1),IG(1+1),I=1,KKK,2)
220 FCRMAT (///,64H THE INDIVIDUAL GRAPH TITLES AND THE CRRRESPONDING
      IVARIABLES ARE ,//,(10X,2A8,4X,2HX(,12,8H) VS. X(,12,1H)))
      GC TO 31
221 WRITE(6,217)
      FCRMAT (///,24H NO GRAPHS ARE REQUIRED )
222 GC TO 31
223 WRITE(6,220)
      FCRMAT (///,52H THE GRAPH TITLE AND THE CRRRESPONDING VARIABLES AR
      LE ,//)
224 WRITE(6,221) KTTITLE(1),KTTITLE(2),IG(1),IG(1+1),I=1,KKK,2)
225 FCRMAT (10X,2A8,4X,2HX(,12,8H) VS. X(,12,1H),/, (30X,2FX(,12,
      8H) VS. X(,12,1H)))
      C
      C
      C
      THIS ENDS THE BOOK-KEEPING. INITIALIZE BEFCRE ENTERING MAIN LCOP.
21 IPAGE = 0
      T = T + 1
      NCPTS = 0
      NUMPTS = 0
      ITITLE(8) = IBLANK
      ITITLE(11) = IBLANK
      ITITLE(12) = IBLANK
      RUN(2) = BT(ARC)
      C(11) = 20.
      C(12) = 5.
      C(13) = DT
      CC 42 I=1,NN
      XC(1) = X(I)
      TC = T
      C(10) = 2.
      RETURN
2000 IF(JJ.EG.0) GO TO 54
      C
      C

```

INT13320
INT13330
INT13350
INT13360
INT13370
INT13380
INT13390
INT13400
INT13410
INT13420
INT13430
INT13440
INT13450
INT13460
INT13470
INT13480
INT13490
INT13500
INT13510
INT13520
INT13530
INT13540
INT13550
INT13560
INT13570
INT13580
INT13590
INT13600
INT13610
INT13620
INT13630
INT13640
INT13650
INT13660
INT13670
INT13680
INT13690
INT13700
INT13710
INT13720
INT13730
INT13740
INT13750
INT13760
INT13770
INT13780
INT13790


```

INCPR = C(11)+0.0000001
C(11) = 20.
IF( MOD (NCPTS,50*INCPR).EQ.0) GC TO 46
IF( MOD (NCPTS,10*INCPR).EQ.0) GC TC 47
IF( MOD (NCPTS,1) IPAGE+1
IPAGE = IPAGE + 1
IF(NR.EQ.1) GO TO 1047
WRITE(6,218) (JTITLE(I),I=1,6),IPAGE,JTITLE(7),(JTITLE(I),I=1,8)
GC TO 47
1047 WRITE(6,1218)(JTITLE(I),I=1,6),IPAGE,(JTITLE(I),I=1,8)
WRITE(6,219)
47 WRITE(6,219)
218 WRITE(6,219)
219 FFORMAT(1H1,///,23X,6A8,7X,5HPAGE,12,14H CF OUTPUT FOR,A8,////,
1218 FFORMAT(1H1,///,23X,6A8,27X,5HPAGE,12,////,21X,4(A8,17X))
219 FFORMAT(1H1, )
48 DC 49 I=1,NN
49 XC(I) = X(I)
TC = T
C(10) = 3.
RETURN
C 50 CC 53 I=1,JJ
C
PR(I) = T
IF(IP(I).NE.0) PR(I)=XC(IP(I))
CONTINUE
53 WRITE(6,220)(PR(I),I=1,JJ)
220 FFORMAT(7X,8E25.5)
54 IF(KK.EQ.0) GO TO 62
INCPR = C(12)+0.0000001
C(12) = 5
IF( MOD (NCPTS, INCPR).NE.0) GO TC 62
DC 57 I=1,NN
57 XC(I) = X(I)
TC = T
C(10) = 4.
RETURN
C 58 CC 61 I=1,KKK
C
GR(I) = T
IF(IG(I).NE.0) GR(I)=XC(IG(I))
CONTINUE
61 IF(KKK.GE.8) GO TC 1610
KKK = KKK + 1
CC 1612 I=KPI,8

```

INT13800
INT13810
INT13820
INT13830
INT13840
INT13850
INT13860
INT13870
INT13880
INT13890
INT13900
INT13910
INT13920

INT13960
INT13970
INT13980
INT13990
INT14000
INT14010
INT14020
INT14030
INT14040
INT14050
INT14060
INT14070
INT14080
INT14090
INT14100
INT14110
INT14120
INT14130
INT14140
INT14150
INT14160
INT14170
INT14180
INT14190
INT14200
INT14210
INT14220
INT14230
INT14240
INT14250
INT14260
INT14270


```

1612 GR(I) = C.NUMPTS + 1
161C NUMPTS = GR(1)
Y1(NUMPTS) = GR(2)
Y2(NUMPTS) = GR(3)
Y3(NUMPTS) = GR(4)
Y4(NUMPTS) = GR(5)
X1(NUMPTS) = GR(6)
X2(NUMPTS) = GR(7)
X3(NUMPTS) = GR(8)
X4(NUMPTS) = NOPTS + 1
62 NUMPTS = NOPTS + 1 GO TO 64
IF(NUMPTS.LT.1000) GO TO 64
WRITE(6,221)
FCRMT(6,221) STOP AT 1000 GRAPH POINTS )
GO TO 91
64 IF(NOPTS.LT.10000) GO TO 66
WRITE(6,222)
FCRMT(6,222) STOP AT 10000 INTEGRATION STEPS )
GO TO 91
66 IF(IPAGE - 15) 69,67,68
67 IF(MOD(NOPTS, 50) = INCPR).NE.0) GO TO 69
68 WRITE(6,223)
FCRMT(6,223) STOP AT 10 PAGES CF OUTPUT )
GO TO 91
69 CC TO 70 I=1;NN
70 CCNTINUE
GO TO 71
71 WRITE(6,224)
FCRMT(6,224) STOP WITH THE ABSOLUTE VALUE CF A DEPENDENT VAR
224 IF(ABLE GREATER THAN 1.0E+18. ,//,57) INTEGRATION PROCEABLY UNSTABLE.
2 TRY A SMALLER STEP SIZE. ,26HNC GRAPHS WILL BE PLCTTED.
GO TO 330
72 IF(TI.GT.TF) GO TO 80
73 IF(TI.LT.TF) GO TO 75
74 WRITE(6,225)
FCRMT(6,225) STOP AT 1000 NORMAL STCP AT FINAL TIME )
GO TO 91
75 IF(TI.GE.TF) GO TO 77
76 CC(13) = DT
GO TO 87
77 IF(TI.GE.TF2) GO TO 79
78 CC(13) = DT2
GO TO 87
79 CC(13) = DT3
GO TO 87
8C IF(TF.GE.T) GO TO 74

```

```

INT14280
INT14290
INT14300
INT14310
INT14320
INT14330
INT14340
INT14350
INT14360
INT14370
INT14380
INT14400
INT14420
INT14440
INT14460
INT14480
INT14490
INT14510
INT14520
INT14540
INT14550
INT14560
INT14570
INT14580
INT14590
INT14600
INT14610
INT14620
INT14630
INT14640
INT14650
INT14660
INT14670
INT14680
INT14690
INT14700
INT14710
INT14720
INT14730
INT14740
INT14750

```



```

      IF(TF1.LT.T) GO TO 76
      IF(TF2.LT.T) 78,79,79
      87 C(10) = 5.
C
      88 CALL RKUTTA (NN,T,X,DT,C,TC,XC,CX)
C
      90 IF(C(10).EQ.6.) RETURN
      T = T + DT
      91 GC TO 2000
      IF(KK.EQ.0) GO TO 330
      IF(MULTIP.NE.0) GC TO 97
C
      PRINT PLCT UP TO 4 INDIVIDUAL CURVES
C
      NUMPTS=-NUMPTS
      DC 310 II=1,KK
      WRITE(6,9998)
      9998 FCRMAT(IH1)
      ITITLE(9)=KTITLE(2*II-1)
      ITITLE(10)=KTITLE(2*II)
      GC TO (311,312,313,314),II
      311 CALL PLCTP(X1,Y1,NUMPTS,0)
      GC TO 310
      312 CALL PLCTP(X2,Y2,NUMPTS,0)
      GC TO 310
      313 CALL PLCTP(X3,Y3,NUMPTS,0)
      GC TO 310
      314 CALL PLCTP(X4,Y4,NUMPTS,0)
      315 WRITE(6,9999) ITITLE
      9999 FCRMAT(IH0,8X,12A8)
      GC TO 330
C
      PLCT DUMMY CURVE ALONG AXES TO SET SCALES FOR MULTIPLE PLOT
C
      97 BIGX = 0.
      BIGY = 0.
      SMLX = 0.
      SMLY = 0.
      DC 1970 I=1,NUMPTS
      XMAX=AMAX1 (X1(I), X2(I), X3(I), X4(I))
      YMAX=AMAX1 (Y1(I), Y2(I), Y3(I), Y4(I))
      XMIN=AMIN1 (X1(I), X2(I), X3(I), X4(I))
      YMIN=AMIN1 (Y1(I), Y2(I), Y3(I), Y4(I))
      IF(BIGX.LT.XMAX) BIGX=XMAX
      IF(BIGY.LT.YMAX) BIGY=YMAX
      IF(SMLX.GT.XMIN) SMLX=XMIN
      IF(SMLY.GT.YMIN) SMLY=YMIN
      1970 CCNTINUE

```



```

TX(1) = 0.
TX(2) = 0.
TX(3) = 0.
TX(4) = 0.
TX(5) = 0.
TY(1) = 0.
TY(2) = 0.
TY(3) = 0.
TY(4) = 0.
TY(5) = 0.
WRITE(6,9998)
ITITLE(9) = KTITLE(1)
ITITLE(10) = KTITLE(2)
NT=-5
CALL FLCTP(TX,TY,NT,1)
MODCUR = 2
DO 410 II=1,MULTIP
  IF (II.EQ.MULTIP) MODCUR=3
  GO TO (411,412,413,414),II
  CALL FLCTP(X1,Y1,NUMPTS,MODCUR)
  GO TO 410
  CALL FLCTP(X2,Y2,NUMPTS,MODCUR)
  GO TO 410
  CALL FLCTP(X3,Y3,NUMPTS,MODCUR)
  GO TO 410
  CALL FLCTP(X4,Y4,NUMPTS,MODCUR)
  CONTINUE
  WRITE(6,9999) ITITLE
C 330 IF(NR.NE.NR) GO TO 1000
  IF(NR.GT.1) GO TO 333
  WRITE(6,226)
  FCURMAT(//,43H THE CNE RUN CALLED FCR HAS BEEN COMPLETED.,//)
226 STOP
227 WRITE(6,227)NR
  FCURMAT(//,5H THE ,11,37H RUNS CALLED FOR HAVE BEEN COMPLETED.,//)
227 STOP
  END

```

```

SUBROUTINE RKUTTA(/NN/,/T/,/X/,/CT/,/C/,/TC/,/XC/,/CX/)
DIMENSION X(30), C(15), XC(30), EX(30), CT(4), AK(4,30)
REAL*8 AK,CT
INCLC=C(10) - 4.0+C.0000001
CT(1) = 0.000
CT(2) = C.500
CT(3) = 0.500

```


BIBLIOGRAPHY

1. Sorokin, P.P. and Stevenson, M.J., "Stimulated Infrared Emission from Trivalent Uranium," Physical Review Letters, v. 5, no. 12, pp. 557-559, 15 December 1960.
2. Brock, E.G., Csavinszky, P., Hormats, E., Nedderman, H.C., Stirpe, D., and Unterleitner, F., "Coherent Stimulated Emission from Organic Molecular Crystals," Journal of Chemical Physics, v. 35, no. 2, pp. 759-760, August 1961.
3. Morantz, D.J., White, B.G. and Wright, A.J.C., "Stimulated Light Emission by Optical Pumping and by Energy Transfer in Organic Molecules," Physical Review Letters, v. 8, no. 1, pp. 23-25, 1 January 1962.
4. Lempicki, A. and Samuelson, H., "Stimulated Processes in Organic Compounds," Applied Physics Letters, v. 2, no. 8, pp. 159-161, 15 April 1963.
5. Sorokin, P.P. and Lankard, J.R., "Stimulated Emission Observed from an Organic Dye, Chloro-aluminum Phthalocyanine," IBM Journal of Research and Development, v. 10, pp. 162-163, March 1966.
6. Sorokin, P.P. and Lankard, J.R., "Flashlamp Excitation of Organic Dye Lasers: A Short Communication," IBM Journal of Research and Development, v. 11, p. 148, March 1967.
7. Schafer, F.P., Schmidt, W. and Volze, J., "Organic Dye Solution Laser," Applied Physics Letters, v. 9, no. 8, pp. 306-309, 15 October 1966.
8. Snively, B.B., "Flashlamp-Excited Organic Dye Lasers," Proceedings of the IEEE, v. 57, no. 8, pp. 1374-1390, August 1969.
9. Snively, B.B. and Schafer, F.P., "Feasibility of CW Operation of Dye Lasers," Physics Letters, v. 28A, no. 11, pp. 728-729, 10 March 1969.
10. Peterson, O.G., Tuccio, S.A. and Snively, B.B., "CW Operation of an Organic Dye Solution Laser," Applied Physics Letters, v. 17, no. 6, pp. 245-247, 15 September 1970.
11. Hercher, M. and Pike, H.A., "Continuous Dye Laser Emission from 5220 to 6570 Angstroms," IEEE Journal of Quantum Electronics, v. QE-7, no. 9, p. 473, September 1971.
12. Hercher, M. and Pike, H.A., "Tuneable Dye Laser Configurations," Optics Communications, v. 3, no. 1, pp. 65-67, March 1971.
13. Hercher, M. and Pike, H.A., "Single Mode Operation of a Continuous Tuneable Dye Laser," Optics Communications, v. 3, no. 5, pp. 346-348, July 1971.

14. Kohn, R.L., Shank, C.V., Ippen, E.P. and Dienes, A., "An Intracavity-Pumped CW Dye Laser," Optics Communications, v. 3, no. 3, pp. 177-178, May 1971.
15. Dienes, A., Ippen, E.P. and Shank, C.V., "High-Efficiency Tuneable CW Dye Laser," IEEE Journal of Quantum Electronics, v. QE-8, no. 3, p. 388, March 1972.
16. Tuccio, S.A. and Strome, F.C., "Design and Operation of a Tuneable Continuous Dye Laser," Applied Optics, v. 11, no. 1, pp. 64-73, January 1972.
17. Strome, F.C. and Tuccio, S.A., "Loss Analysis and Design Improvement for a Continuous Dye Laser," IEEE Journal of Quantum Electronics, v. QE-9, no. 2, pp. 230-235, February 1973.
18. Shank, C.V., Bjorkholm, J.E. and Kogelnik, H., "Tunable Distributed-Feedback Dye Laser," Applied Physics Letters, v. 18, no. 9, pp. 395-396, 1 May 1971.
19. Chandra, S., Takeuchi, N. and Hartmann, S.R., "Prism-dye Laser," Applied Physics Letters, v. 21, no. 4, pp. 144-146, 15 August 1972.
20. Ippen, E.P. and Shank, C.V., "Evanescent-Field-Pumped Dye Laser," Applied Physics Letters, v. 21, no. 7, pp. 301-302, 1 October 1972.
21. Bloom, Arnold M., "CW Pumped Dye Lasers," Coherent Radiation Technical Bulletin, 1972.
22. Sorokin, P.P., Lankard, J.R., Moruzzi, V.L. and Hammond, E.C., "Flashlamp-Pumped Organic-Dye Lasers," The Journal of Chemical Physics, v. 48, no. 10, pp. 4726-4741, 15 May 1968.
23. Dewey, C.F. and Hocker, L.O., "Infrared Difference-Frequency Generation Using a Tunable Dye Laser," Applied Physics Letters, v. 18, no. 2, pp. 58-60, 15 January 1971.
24. Bradley, D.J., Nicholas, J.V. and Shaw, J.R.D., "Megawatt Tunable Second Harmonic and Sum Frequency Generation at 280 Nanometers from a Dye Laser," Applied Physics Letters, v. 19, no. 6, pp. 172-173, 15 September 1971.
25. Hansch, T.W., "Repetitively Pulsed Tunable Dye Laser for High Resolution Spectroscopy," Applied Optics, v. 11, no. 4, pp. 895-898, April 1972.
26. Baardsen, E.L. and Terhune, R.W., "Detection of OH in the Atmosphere Using a Dye Laser," Applied Physics Letters, v. 21, no. 5, pp. 209-211, 1 September 1972.
27. Beiser, A., Perspectives of Modern Physics, McGraw-Hill, 1969.
28. Lower, S.K. and El-Sayed, M.A., "The Triplet State and Molecular Electronic Processes in Organic Molecules," Chemical Review, v. 66, no. 2, pp. 199-241, April 1966.

29. Condon, E.U., "The Franck-Condon Principle and Related Topics," American Journal of Physics, v. 15, no. 5, pp. 365-374, September-October 1947.
30. Kasha, M., "Characterization of Electronic Transitions in Complex Molecules," Discussions of the Faraday Society, no. 9, pp. 14-19, 1950.
31. Snavely, B.B. and Peterson, O.G., "Experimental Measurement of the Critical Population for the Dye Solution Laser," IEEE Journal of Quantum Electronics, v. QE-9, no. 10, pp. 540-545, October 1968.
32. Yariv, A. and Gordon, J.P., "The Laser," Proceedings of the IEEE, v. 51, no. 1, pp. 4-29, January 1963.
33. McColgin, W.C., Webb, J.P., Eberly, J.H. and Peterson, O.G., "Organic Dye Laser Threshold," Journal of Applied Physics, v. 42, no. 5, pp. 1917-1928, April 1971.
34. Atkinson, J.B. and Pace, F.P., "The Spectral Linewidth of a Flashlamp-Pumped Dye Laser," IEEE Journal of Quantum Electronics, v. QE-9, no. 6, pp. 569-574, June 1973.
35. Maydan, D., "Fast Modulator for Extraction of Internal Laser Power," Journal of Applied Physics, v. 41, no. 4, pp. 1552-1559, 15 March 1970.
36. Sorokin, P.P., Lankard, J.R., Hammond, E.C. and Moruzzi, V.L., "Laser-Pumped Stimulated Emission from Organic Dyes: Experimental Studies and Analytical Comparisons," IBM Journal of Research and Development, v. 11, pp. 130-147, March 1967.
37. Bass, M., Deutsch, T.F., and Weber, M.J., "Frequency-and Time-Dependent Gain Characteristics of Laser-and Flashlamp-Pumped Dye Solution Lasers," Applied Physics Letters, v. 13, no. 4, pp. 120-124, 15 August 1968.
38. Bass, M. and Weber, M.J., "Frequency-and Time-Dependent Gain Characteristics of Dye Lasers," IEEE Journal of Quantum Electronics, v. QE-5, no. 4, pp. 175-187, April 1969.
39. Keller, Richard A., "Effect of Quenching of Molecular Triplet States in Organic Dye Lasers," IEEE Journal of Quantum Electronics, v. QE-6, no. 7, pp. 411-416, July 1970.
40. Pappalardo, R., Samuelson, H., and Lempicki, A., "Calculated Efficiency of Dye Lasers as a Function of Pump Parameters and Triplet Lifetime," Journal of Applied Physics, v. 43, no. 9, pp. 3776-3787, September 1972.
41. Streifer, W. and Salt, P., "Transient Analysis of an Electronically Tunable Dye Laser-Part II: Analytic Study," IEEE Journal of Quantum Electronics, v. QE-9, no. 6, pp. 563-569, June 1973.

42. Buettner, A.V., Shavely, B.B. and Peterson, O.G. in Molecular Luminescence, edited by E.C. Lim, p. 403, Benjamin, New York, 1969.
43. Mack, M.E., "Measurement of Nanosecond Fluorescence Decay Times," Journal of Applied Physics, v. 39, pp. 2483-2485, April 1968.
44. Bass, M. and Steinfeld, J.I., "Wavelength Dependent Time Development of the Intensity of Dye Solution Lasers," IEEE Journal of Quantum Electronics, v. QE-4, no. 2, pp. 53-58, February 1968.
45. Private Communication with Spectra Physics in February 1973.
46. Jacobs, R.R., Samuelson, H. and Lempicki, A., "Losses in CW Dye Lasers," Journal of Applied Physics, v. 44, no. 1, pp. 263-272, January 1973.

INITIAL DISTRIBUTION LIST

	No. Copies
1. Defense Documentation Center Cameron Station Alexandria, Virginia 22314	2
2. Library, Code 0212 Naval Postgraduate School Monterey, California 93940	2
3. Asst. Professor J. P. Powers, Code 52 Po Department of Electrical Engineering Naval Postgraduate School Monterey, California 93940	1
4. LCDR Gerald W. Snyder, USN 1937 E. Ivy Avenue Saint Paul, Minnesota 55119	1
5. Dr. Richard S. Hughes, Code 6043 Naval Weapons Center China Lake, California 93555	1
6. Mr. Jim Jernigan, Code 6043 Naval Weapons Center China Lake, California 93555	1

20. (cont'd)

agreement is obtained within the limits of the values of the parameters used and the assumptions made in formulating the model.

3 NOV 74

3401

Thesis
S6627 Snyder
c.1

146134

The wave length spec-
trum shift of a cavity-
dumped argon laser-
pumped Rhodamine 6-G
organic-dye laser.

3 NOV 74

3401

Thesis
S6627 Snyder
c.1

146134

The wave length spec-
trum shift of a cavity-
dumped argon laser-
pumped Rhodamine 6-G
organic-dye laser.

thesS6627

The wavelength spectrum shift of a cavit



3 2768 001 00515 0

DUDLEY KNOX LIBRARY